In silico modeling of the induction of apoptosis by Cryptotanshinone in osteosarcoma cell lines

Radhika Saraf, *Student Member, IEEE,* Aniruddha Datta, *Fellow , IEEE,* Chao Sima, Jianping Hua, Rosana Lopes, Michael L. Bittner, Tasha Miller, and Heather M. Wilson-Robles

Abstract—Osteosarcoma (OS) is the most common primary malignant bone tumor of both children and pet canines. Its characteristic genomic instability and complexity coupled with the dearth of knowledge about its etiology has made improvement in the current treatment difficult. We use the existing literature about the biological pathways active in OS and combine it with the current research involving natural compounds to identify new targets and design more effective drug therapies. The key components of these pathways are modeled as a Boolean network with multiple inputs and multiple outputs. The combinatorial circuit is employed to theoretically predict the efficacies of various drugs in combination with Cryptotanshinone. We show that the action of the herbal drug, Cryptotanshinone on OS cell lines induces apoptosis by increasing sensitivity to TNF-related apoptosis-inducing ligand (TRAIL) through its multi-pronged action on STAT3, DRP1 and DR5. The Boolean framework is used to detect additional drug intervention points in the pathway that could amplify the action of Cryptotanshinone.

Index Terms—Boolean Networks; Drug Targets; Simulation and Modeling; Cancer; Osteosarcoma; Cryptotanshinone

---

✦

---

1 INTRODUCTION

OSTEOSARCOMA(OS) is the most common primary malignant bone tumor of both children and pet canines [1]. Approximately 800 new cases of OS are diagnosed in people each year and more than half of those are in children or adolescents. The incidence is approximately 8-10 times higher in pet dogs than in children [1]. Genetically, these two diseases are the same in humans and canines [2], [3], [4]. They share dysregulation of many of the same pathways that lead to metastasis in over 80% of affected individuals treated with surgery alone [2], [3], [4]. The bone tumor is found in areas of rapid cell growth that are susceptible to mitotic errors and oncogenic agents [5]. Alterations in the p53 and Rb tumor suppressor pathway are common in OS patients, however conventional drug therapies that target these tumor suppressor pathways have had little success in the late stages of the clinical trials [6]. There is a need to identify key intervention points in the biological pathways associated with OS that could help design effective drug therapies and ensure robust cell death of cancer cells.

The complete etiology of OS is unclear and there is no conclusive evidence to indicate which genetic mutations or pathway alterations could be responsible for the develop-

ment of the bone cancer [7]. There is a large set of potential candidate genes which must be evaluated to characterize molecular targets in order to develop new strategies [8], [9]. Our approach to narrow the search space is two-pronged; one, we investigate the drugs that have been successful in clinical trials and evaluate their targets as potential intervention points and two, we study OS in dogs to identify statistically significant mutations that could be associated with the bone cancer. The higher incidence and more rapid disease progression seen in pet dogs allows for faster and more cost effective data collection making them an excellent model for studying this disease to the mutual benefit of both species [10].

Recent success in OS therapy has been through trials that target the stemness pathways, namely Wnt/β-Catenin and Hedgehog pathways through the use of natural compounds [9]. Sulforaphane is one of the natural compounds being used to treat OS cell lines; the drug increases the expression of death receptors and induces tumor necrosis factor (TNF)–related apoptosis-inducing ligand (TRAIL) apoptosis [8], [11]. TRAIL therapy is a therapeutic strategy that inhibits tumor growth and increases chances of survival in preclinical studies for OS. Since TRAIL-induced cell death is known to only kill cancer cells and not affect normal cells, it is one of the popular emerging strategies in pediatric cancer care and another pathway that warrants investigation [11], [12]. In this work, we model the stemness pathways and their interaction with the various pathways involved in TRAIL sensitivity for OS.

The gene expression patterns of OS in humans and dogs are very similar, making the dog a valid model for OS research [2], [3], [4]. An evaluation of OS in dogs tells us that the pathways involved in the glutathione and aspartate metabolism may have an important part to play in the early spread of this cancer [2]. We will incorporate the relevant interconnections and cross talk with the metabolic pathways

- R. Saraf and A. Datta are with the Department of Electrical and Computer Engineering, Texas A&M University, College Station, TX and the TEES-AgriLife Center for Bioinformatics and Genomic Systems Engineering (CBGSE).
  E-mail: saraf.radhika@tamu.edu
- C. Sima, J. Hua and R. Lopes were with TEES-AgriLife Center for Bioinformatics and Genomic Systems Engineering (CBGSE), College Station, TX.
- M. Bittner was with Translational Genomics Research Institute, Phoenix, AZ and the TEES-AgriLife Center for Bioinformatics and Genomic Systems Engineering (CBGSE) .
- T. Miller and H. Wilson-Robles are with the Department of Small Animal Medicine and Surgery, College of Veterinary Medicine, Texas A&M University, College Station, TX.

into our model.

In this work, we study the action of Cryptotanshinone (CT), a derivative of the herb Salvia milthorrhiza Bunge and its effect on OS pathways. CT is a known STAT3 inhibitor and has been used to eradicate tumor-initiating cells in other cancers [13], [14], [15], [16]. Additionally, CT is known to be effective in increasing TRAIL cytotoxicity by upregulating death receptor 5 (DR5) and inducing cell death in cancer cells [17], [18]. Through its action on dynamin-related protein 1 (DRP1), CT controls mitochondrial function which could inhibit OS cell growth [19]. This makes CT a promising candidate drug for treatment of OS.

2 MATERIALS AND METHODS

2.1 Boolean Network Modeling

We use a Boolean network model to capture the causal interconnections between the different genes from the different biological pathways. In the paradigm of Boolean network modeling, each gene is a node and its direct interaction with another gene is represented as an edge. Gene expression is binarily quantized: a gene, if expressed is considered to be ON (State 1) and if not expressed, is considered to be OFF (State 0). If two or more genes interact to activate or inhibit a third gene, such relationships are modelled with the use of logic gates. The genetic regulatory network can be represented as a multi-input multi-output (MIMO) digital logic circuit [20].

The static Boolean network considered in this work is subject to a certain set of inputs whose effect on the network can be evaluated through a set of outputs; the input and output vectors are given in Eq. 1 and Eq. 2 below. The inputs are a mix of growth factors, interleukins, interferons and stress signals which activate the pathways relevant to the pathogenesis of OS. The value of these inputs manipulate cell growth and death by controlling the state of the nodes downstream. The outputs are a set of genes that give information about cell death or apoptosis. The outputs can be classified into two categories: pro-apoptotic and anti-apoptotic, which promote and inhibit cell death respectively. The Table. 1 shows this classification of outputs. The fate of the cell depends on the value of these apoptotic factors.

$$\text{Inputs} = [\text{IGF}, \text{TRAIL}, \text{CaLM}, \text{EGF}, \text{TNF}\alpha, \quad (1)$$
$$\text{IL6}, \text{TGF}\beta, \text{IFN}, \text{Hh}, \text{WNT}, \text{cAMP}, \text{ROS}]$$

$$\text{Outputs} = [\text{BAKX}, \text{BAD}, \text{CASP8}, \text{CASP12}, \text{BID}, \quad (2)$$
$$\text{BIM}, \text{STING}, \text{DRP1}, \text{BCL2}, \text{BCLxL},$$
$$\text{MCL1}, \text{XIAP}, \text{XBP1}, \text{survivin}, \text{EPO}, \text{A1}]$$

Genetic aberrations in cancer cells are responsible for abnormal upregulation or downregulation of their downstream targets. These anomalies of tumor cells can be represented as stuck-at faults in the Boolean circuit [29]. When a node in the circuit is permanently set to a fixed value of either zero or one, a stuck-at fault is said to occur. An overexpressed gene can be modeled as a stuck-at-1 fault. For example, STAT3 is activated in many cancers and remains phosphorylated even in the presence of inhibitors like PTP.

TABLE 1
Apoptotic Factors. Pro-apoptotic factors increase the chances of cell death and anti-apoptotic factors increase the chances of survival.

Pro-apoptotic factors	Anti-apoptotic factors
BAK/BAX [21], [22]	BCL2 [21], [22]
BAD [21], [22]	BCLxL [21], [22]
CASP8 [23]	MCL1 [24]
CASP12 [25]	XIAP [21], [22]
BID [23]	XBP1 [25]
BIM [21], [22]	survivin [26], [26], [27]
STING [28]	EPO [26], [26], [27]
DRP1 [19]	A1 [21], [22]

TABLE 2
Faults in the Boolean network. The type of fault indicates whether a gene is overexpressed (Stuck at 1) or silenced (Stuck at 0).

Fault	Type
CXCR4	Stuck at 1
SLC1A3	Stuck at 0
IL8	Stuck at 0
MDM2	Stuck at 1
p53	Stuck at 0
PTEN	Stuck at 0
STAT3	Stuck at 1

This dysregulation of STAT3 can be modeled as a stuck-at-1 fault [20]. The effect of such a fault can be corrected by using a drug as shown in the Fig. 1. A stuck-at-0 fault occurs when the node or gene is permanently inactive independent of the signals upstream. For instance, a mutated p53 gene remains inactive despite being phosphorylated due to cellular DNA damage. This situation can be corrected through the use of drugs as can be seen in Fig. 2.

We consider a total of 7 faults in our network. PTEN, p53, MDM2 and CXCR4 mutations are commonly found in OS cell lines; PTEN and CXCR4 faults can lead to a decrease in TRAIL sensitivity [6], [7], [9], [30], [31]. OS cell survival and drug resistance can be attributed to STAT3 overexpression, which can be characterized as a stuck-at-1 fault [13]. Furthermore, the study of canine gene expression identifies SLC1A3 and IL8 as the two mutations that could be responsible for OS progression in humans and dogs [2]. The faults and their corresponding types are displayed in Table 2 and the fault vector can be seen in Eq. 3. The components in the fault vector are either one or zero depending on whether a particular fault is present or not. A one in the fault vector denotes a stuck-at-0 or stuck-at-1 fault, whichever is applicable for that particular gene. For example, if the fault vector is $[0, 0, 0, 0, 0, 0, 1]$, this implies that the STAT3 gene is mutated. Since it is a stuck-at-one type of fault, it means that STAT3 is being constitutively expressed.

$$\text{Faults} = [\text{CXCR4}, \text{SLC1A3}, \text{IL8}, \text{MDM2}, \text{p53}, \text{PTEN}, \text{STAT3}] \quad (3)$$

The drugs with their respective intervention points are shown in Table 3 and the components of the drug vector are given in Eq. 4.
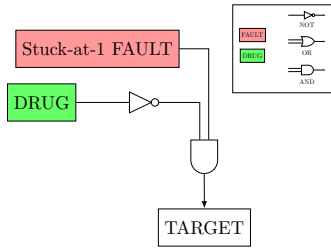
Fig. 1. Boolean Representation of a Stuck-at-1 fault. The drug acts on the target to compensate for the effect of the fault.
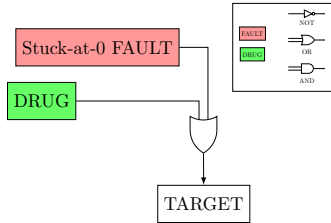

Fig. 2. Boolean Representation of a Stuck-at-0 fault. The drug acts on the target to compensate for the effect of the fault.

TABLE 3
Drugs and the corresponding targets.

Abbreviation	Drug	Target
Cry	Cryptotanshinone	STAT3, DR5 [17], DRP1 [19]
Ly	LY294002	PI3K [29]
Lap	Lapatinib	EGFR [3]
NT	NT157	PTP [32]
SH	SH-4-54	STAT3 [33]
Tem	Temsirolimus	mTOR [34]
U0	U0126	MEK1 [29]
PX	PX-478	HIF1α [35]

$$\text{Drugs} = [\text{Cry}, \text{Ly}, \text{Lap}, \text{NT}, \text{SH}, \text{Temsirolimus}, \text{UO126}, \text{PX}] \quad (4)$$

A one in the ith column of the drug vector indicates that the ith drug is applied and vice versa. We evaluate combinations of Cryptotanshinone with the other drugs, since a major goal of this work is to evaluate CT's action on OS cells. Since there are seven other drugs in the vector, a total of 2^7 drug combinations were tested. For instance, the drug vector $[1, 0, 0, 0, 0, 0, 0, 0]$ indicates that only Cryptotanshinone is applied.

2.2 Biological Pathways in osteosarcoma

In order to construct a Boolean network for TRAIL sensitivity in OS, we must evaluate the pathways active in most cancers and identify the subset of interconnections relevant to OS development. To narrow the scope of the search, we focus on pathways commonly altered in canine OS as well as pathways targeted by drugs in successful clinical trials for OS. The candidate biological pathways for OS, namely cell survival and growth (PI3k/mTOR, MAPK/ERK), angiogenesis (JAK/STAT), DNA Damage (p53), immune system (KEAP1/NRF2),

inflammation(NKκB), hypoxia (H1F1α), stemness (Wnt/β-Catenin and Hedgehog) and the metabolic pathways, are all well documented [20], [26], [27], [36]. We will model the genetic interactions in the candidate pathways and derive interconnections between the pathways based on our interpretation of different research papers. For clarity of exposition, the entire biological network has been divided into six components depicted in Fig 3a through Fig 4c.

First, we consider the cell survival pathways [26], [27], [29], [32], [34], [36], [37], [38] in Fig 3a; this figure shows the activity points of many conventional drugs. Cancer cells hijack the cell survival mechanism to evade cell death and to promote the growth of the tumor. The PI3K-mTOR pathway is mutated in certain OS cells and is implicated in drug resistance as well as TRAIL resistance [30], [31].

The stemness pathways are modeled in Fig. 3b. Mesenchymal cells split to form osteoblasts (or young bone cells) and could be responsible for osteosarcoma pathogenesis [13]. The Wnt and Hedgehog pathways are considered in our model since they regulate the stemness factors required for a mesenchymal stem cell to become a bone cell. The figure also shows the cytokine signalling pathway TGFβ and how it promotes cell growth in osteoblasts [8], [39]. Additionally, natural compounds such as Reservetrol, Apigenin and Cyclopamine that target the stemness pathways have shown promising results in osteosarcoma clinical trials [9].

Fig. 3c shows the interconnections between the endoplasmic reticulum stress-activated pathway and cellular damage and their cumulative effect on the glutathione metabolism. The hypoxic (low oxygen) conditions associated with cancer cause endoplasmic reticulum stress to initiate the unfolded protein response; the low oxygen condition also initiates the switch to anaerobic metabolism [25]. JNK regulates p53 and IL8, both of which are mutated in osteosarcoma [2], [40]. Cellular damage in cancer cells goes unchecked, which can lead to further genetic instability in the tumor cells. CHK1 and p53 are components of the cellular damage and repair mechanism [24]. The interconnection of the p53 pathway with the glutathione (GSH) metabolism can help us understand what role SLC1A3 plays in OS cells [41], [42]. Both IL8 and SLC1A3 have been implicated in genetic studies of canine OS [2].

Hypoxia and angiogenesis pathways are displayed in Fig. 4a, the gene STAT3 and its influence on the immune system, inflammation, angiogenesis as well as hypoxia can be studied in this figure. We can also observe the crosstalk of the mTOR pathway with the JAK/STAT pathway [38] in the figure. Endoplasmic reticulum stress releases PERK, which activates STAT3 [43]. STAT3, in turn, activates anti-apoptotic factor MCL1 [24] as well as COX2 in the inflammation pathway [23]. Inhibition of STAT3 could be crucial to restoring TRAIL sensitivity [18], especially given its interaction with CHOP, a promoter of extrinsic death receptors [44]. HIF1α is expressed when hypoxic conditions exist in cells [45]. Both hypoxia and endoplasmic reticulum stress have an effect on the immune system pathway KEAP/NRF2 [28], [46], [47].

Fig. 4b and Fig. 4c show the extrinsic and mitochondrial apoptotic pathways respectively. The induction of TRAIL apoptosis by CT can be seen in Fig. 4b. TRAIL sensitivity
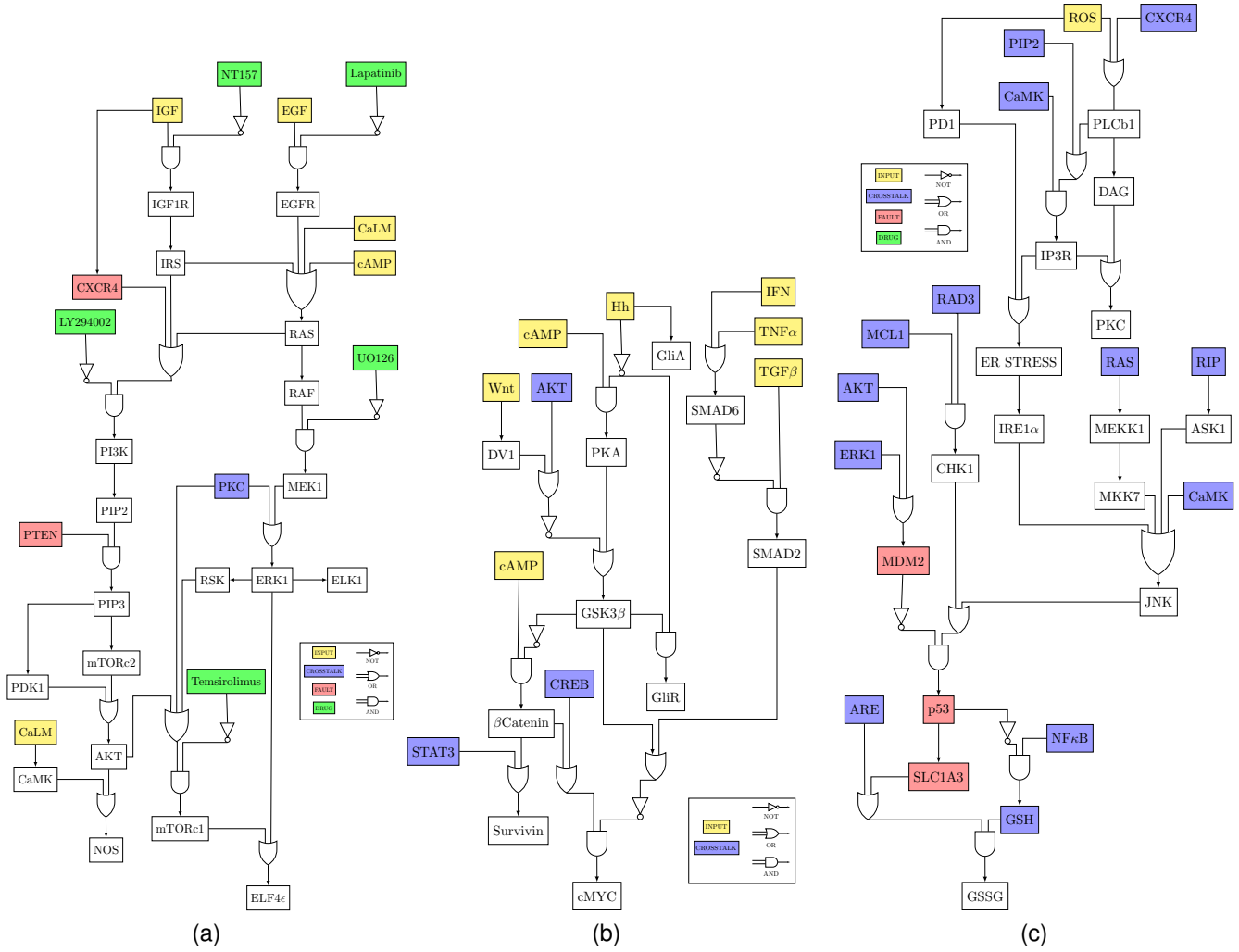
Fig. 3. (a) Boolean network for Cellular Survival Pathways in osteosarcoma. (b) Boolean network for Stemness Pathways in osteosarcoma. (c) Boolean network for Endoplasmic Reticulum Stress-related Pathways and their interconnections with cellular damage and the Glutathione metabolism.

depends on the expression of the death receptor, DR5 [17], [48]. STAT3, PI3K and others can cause TRAIL resistance by affecting the genes upstream of DR5. The interleukin IL8 is expressed downstream in the TRAIL pathway and can cause TRAIL resistance [2], [23], [40], [49]. The extrinsic apoptosis factor CASP8 eventually leads to mitochondrial apoptosis.

The entire Boolean Network model is available in the code associated with the project (refer to Appendix 1).

3 RESULTS AND DISCUSSION

In this section, we predict the cell death in OS cells for various combinations of inputs, drugs and faults. Next, we compare the predicted values of cell death with the results of biological experiments on OS cells subject to different drug combinations. Finally, we predict theoretical drug efficacies for all possible combinations of drugs and faults considered in this paper.

We ran simulations under different combinations of drugs and faults to predict the theoretical drug efficacies of drug combinations with Cryptotanshinone. The efficacy of a cancer drug is proportional to its ability to stop cell proliferation and induce cell death in cancerous cells. To predict the

theoretical efficacy of a cancer drug, we measure its effect on apoptotic factors to gauge the degree of apoptosis. The metric used to calculate the degree of apoptosis is given in Eq. 5.

$$\text{Apoptosis Ratio} = \frac{\sum \text{Pro-Apoptotic factors}}{\sum \text{Anti-Apoptotic factors}} \quad (5)$$

The apoptosis ratio measures the relative change in cell death for each different set of inputs. The active faults and drugs will also affect the apoptosis ratio. During every simulation, a particular combination of drugs and faults will be fed to the Boolean network, which in turn activates or inhibits the corresponding apoptotic factors. We calculate arithmetic means of the pro- and anti-apoptotic factors and obtain the apoptosis ratio. The apoptosis ratio will be treated as the predicted drug efficacy for a particular drug combination.

3.1 Experimental Results

Cellular apoptosis is tracked using high-content fluorescent protein reporter imaging with the previously immortalized ABRAMS canine OS cell line to study how it reacts to
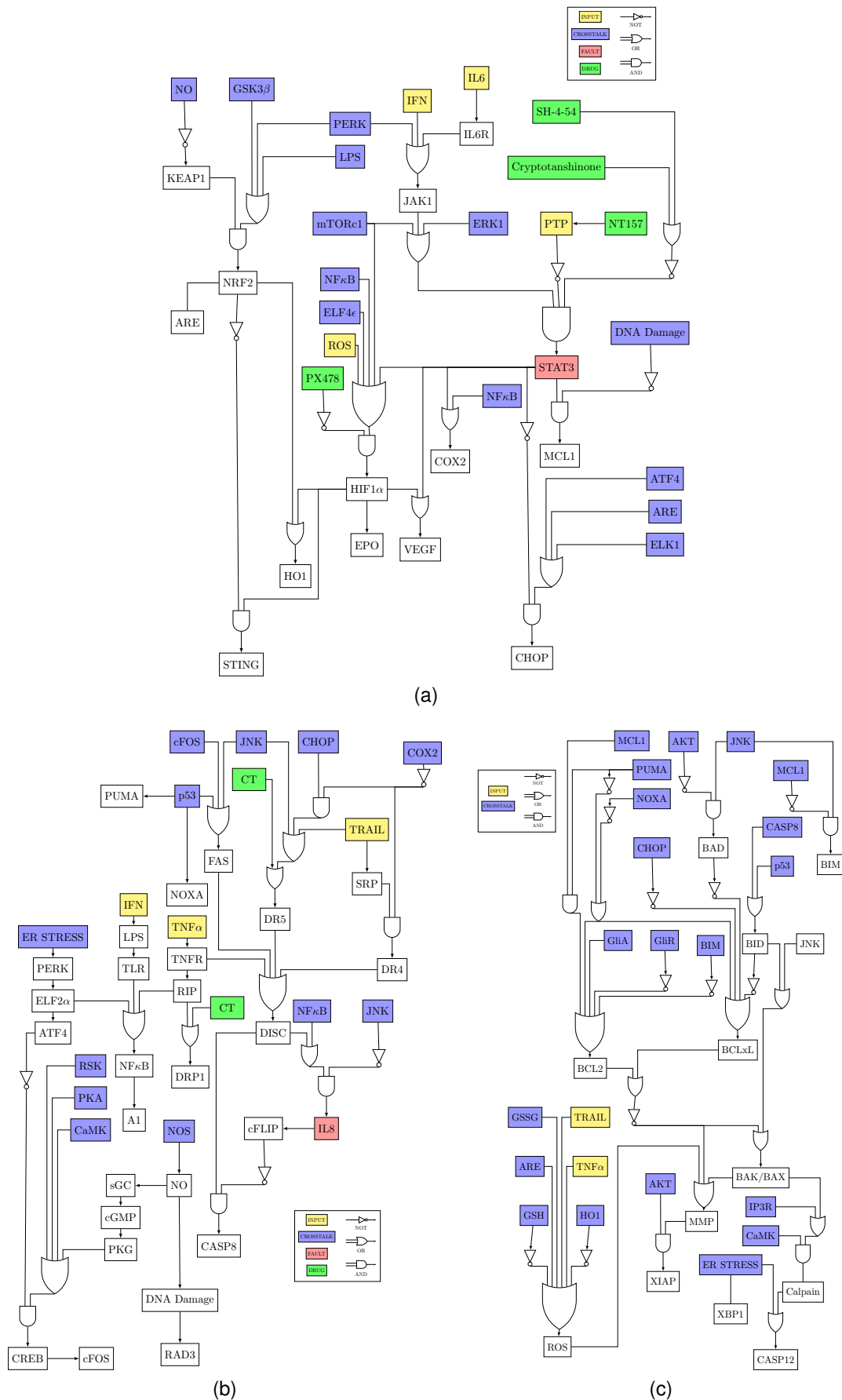
Fig. 4. (a) Boolean network for Hypoxia and Angiogenesis pathways and their cross-talk with the immune system. (b) Boolean network for Extrinsic Apoptosis in osteosarcoma. (c) Boolean network for Intrinsic Apoptosis in osteosarcoma.
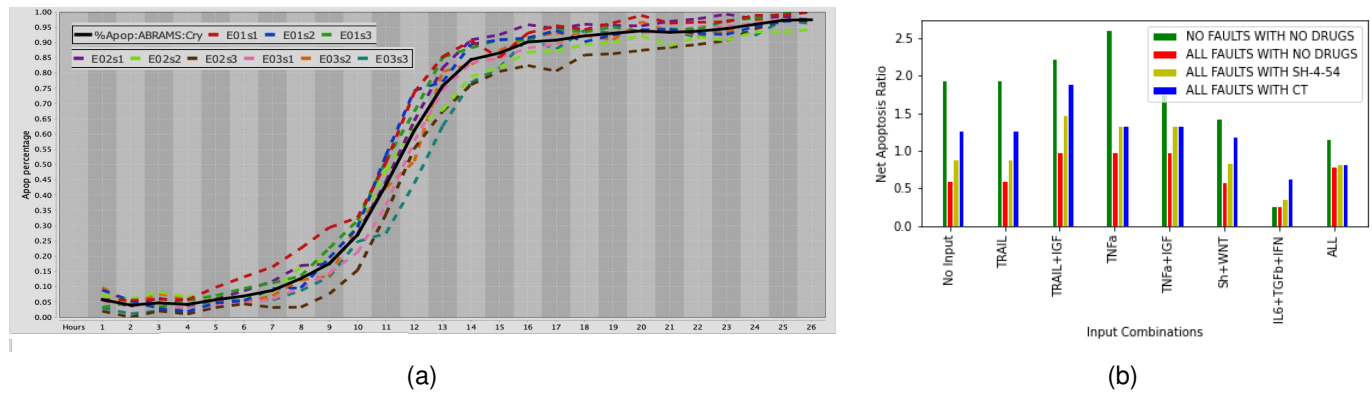
(a) (b)

Fig. 5. (a) The induction of cell death in ABRAMS cells by Cryptotanshinone is displayed in this plot. Each dotted curve represents a replicate and the solid curve represents the final plot for average cellular apoptosis versus time. (b) The predicted values of apoptosis ratio when the Boolean Network is subject to different inputs. For every input, we compare how the apoptosis ratio changes with the presence of faults and drugs.

different combinations and concentrations of drugs. A two-part data processing technique is applied to extract the cell dynamics from the images. First, morphological image processing is performed on the fluorescent images to recognize individual cells and quantify their transcription activity levels. Second, an algorithm for data representation summarizes the results into expression profiles in order to facilitate further evaluation. The details of this method have been outlined in a previous publication [50]. Each experiment has nine replicates and the result is obtained by finding the average of the replicates. The final result is represented by a single plot of cellular apoptosis versus time for a given drug combination. Fig 5a shows the average cellular apoptosis with all nine replicates for Cryptotanshinone acting on ABRAMS OS cells.

3.2 Fixing the parameters of the Boolean Network

The Boolean network can be manipulated by changing the values of inputs, drugs and faults. We wish to fix the parameters of the Boolean network such that it represents a TRAIL resistant network of OS cells.

We record the values of apoptosis ratios for different values of input to the Boolean network. Every input activates its corresponding pathway. For instance, the input Hh when set to one activates the Hedgehog pathway. In Fig 5b, we have plotted the outputs of the Boolean network for different inputs and different values of drugs and faults.

- 'NO FAULTS' - When the cancer cell network has no faults, it acts like the network of a normal bone cell.
- 'NO DRUGS' - When the cancer cell network has no drugs, it represents the untreated condition of the OS cells. This serves as the control against which we can compare the effect of the drugs.
- 'NO FAULTS WITH NO DRUGS' - This represents the highest value of apoptosis that the Boolean network can achieve given a particular set of input conditions.
- 'ALL FAULTS WITH NO DRUGS' - This represents the lowest level of apoptosis that the Boolean network can achieve without drug intervention given a particular set of input conditions..
- 'WITH CT' - We are examining the effect of Cryptotanshinone or CT on OS cells.

- 'WITH SH-4-54' - CT and SH-4-54 are both STAT3 inhibitors. We can compare the efficacy of the two drugs to see if one is better than the other.

If we compare 'NO FAULTS NO DRUGS' to 'ALL FAULTS NO DRUGS', we can see that the cancer cell has lower apoptosis than the normal cell for all input combinations. This implies that the genetic mutations decrease the amount of apoptosis and allow cancer cells to survive. Then, for a drug to be effective it has to be able to restore apoptosis to its normal value or fault-free value. If we observe the 'ALL FAULTS WITH SH-4-54' bars, we can see that SH-4-54 is able to increase the cell death despite the presence of faults, but it is not able to achieve the level of fault-free apoptosis. Similarly, from the 'ALL FAULTS WITH CT' bars, we can say that CT is more effective than SH-4-54.

In Fig 5b, we compare 8 different input conditions. The 'No Input' condition is when none of the inputs to the OS pathways are active. The apoptosis values of this condition are almost similar to the 'TRAIL' condition. This could be attributed to TRAIL resistance in OS cells. TRAIL resistance is observed in OS cells and is said to occur when an active TRAIL input is unable to induce apoptosis in cancer cells [51]. IGF activates the PI3K/mTOR pathway which has been implicated in decreasing TRAIL cytotoxicity [31]. The involvement of the IGF pathway in TRAIL resistance is not evident from this figure and it warrants further investigation.

The other input conditions are shown to elucidate the effectiveness of CT in the presence of different combinations of interleukins, growth factors and other extracellular signals.

- 'TNFa' - One of the extrinsic apoptosis pathways, TNFα causes a high amount of apoptosis in normal cells.
- 'TNFa + IGF' - The PI3K/mTOR pathway decreases apoptosis as expected.
- 'Hh + WNT' - This represents the apoptosis caused by the stemness pathways.
- 'IL6 + TGFb + IFN' - This represents the apoptosis caused by the cytokines of the immune system.
- 'ALL' - This represents the apoptosis caused by the simultaneous activation of all the pathways in the Boolean network.

TABLE 4
Interpretation of the numerical values of theoretical drug efficacies for the input condition 'TRAIL+IGF'.

Term	Theoretical Drug Efficacy
Fault-free apoptosis ratio	2.23
Untreated apoptosis ratio	0.9
Low theoretical efficacy	1.0 to 2.0
High theoretical efficacy	> 2.0
Not effective	< 1.0

We fix the values of the inputs for all the simulations as $[1, 1, 0, 0, 0, 0, 0, 0, 0, 0, 0, 0, 0, 0]$, where the IGF and TRAIL inputs are active, since TRAIL sensitivity is of us interest to us. TRAIL sensitivity is the ability of a cancer cell to respond to death signals. We wish to investigate the role the IGF pathway plays in TRAIL resistance in OS cells.

While running the first four simulations, we assume that all faults are active, i.e. the fault vector is $[1, 1, 1, 1, 1, 1, 1]$. All the faults considered in this paper are strongly associated with OS. The genetic signatures of canine and human OS cells are similar and we have used the literature to identify genetic mutations that have relevance for both human and OS therapy.

Note that the value of fault free apoptosis for the input condition 'TRAIL + IGF' is 2.23 and the untreated condition for this input combination in the presence of faults ('ALL FAULTS WITH NO DRUGS') is 0.9. For all the simulations in this section, if the value of a drug combination is greater than 1, then it successfully induces apoptosis in OS cells. However, an effective drug combination should have a theoretical efficacy close to 2.23 so as to correct for the faults in the cancer cell networks. Table 4 provides a key to understand the simulation results better.

3.3 CT is effective at restoring TRAIL sensitivity

First, we compare the action of Cryptotanshinone alone with the action of the PI3K inhibitor LY294002. Fig. 6a shows the simulated effect of the drugs CT and LY294002 on the Boolean network. The 'Untreated' condition is simulated by passing a drug vector of zeros and can serve as a control for the experiment. The Boolean network subject to Cryptotanshinone outputs a greater apotosis ratio than the one subject to LY294002.

The cellular apoptosis occurring in ABRAMS OS cells with respect to time is displayed in Fig 6c. The Y-axis shows the apoptotic fraction, which corresponds to the percentage of apoptosis occurring in the cell line in the given time. The curve in Fig. 6c shows the effect of CT and LY294002 on OS cells. It is clear from the Fig. 6c that Cryptotanshinone is more effective than LY294002 in inducing apotosis. The area under the curve for each of the curves in Fig. 6c is plotted in Fig. 6b as a bar graph for ease of comparison. Upon comparison of Fig. 6a and Fig. 6b, it is evident that the two graphs are similar. The simulation shows us that CT can induce apoptosis on its own, whereas the inhibition of PI3K alone is not sufficient to restore TRAIL cytotoxicity.

3.4 Inhibition of the PI3K/mTOR pathway boosts CT's action

Next, we test the combination of Cryptotanshinone with one drug at a time. The output of the Boolean network gives us the predicted apoptosis ratio for the drug combinations and is shown in Fig 7a. From Fig 7a, we can see that LY294002, the PI3K inhibitor in combination with CT is the best performing combination. We can also see that all the combinations lead to high values of the apoptosis ratio.

The cellular apoptosis occurring in ABRAMS OS cells with these conditions is displayed in Fig 7c. We have five drugs in different concentrations mixed with equal dosage of Cryptotanshinone. The curve in Fig. 7c shows how all the drug combinations successfully lead to apoptosis. Note that since every combination has Cryptotanshinone as a component, it could imply that Cryptotanshinone is responsible for the effectiveness of the drug cocktail. We can see that the combination of CT with Temsirolimus, the MTOR inhibitor is the most effective. The area under the curve for each of the curves in Fig. 7c is plotted in Fig. 7b as a bar graph for ease of comparison. Both Fig. 7b and Fig. 7a seem to indicate that the inhibition of PI3K/mTOR pathway amplifies the effect of CT and helps overcome TRAIL resistance.

3.5 HIF1α is a key intervention point in OS pathways

The third experiment was performed with Cryptotanshinone with two drugs at a time. All the drug combinations in this experiment have Cryptotanshinone and HO-3867 (a STAT3 inhibitor) in the mix. Fig 8a shows the theoretical efficacies of the drug combinations. The simulation results predict that the combination of CT with PX-478 will be more effective than CT alone. The drug combinations CT, CT + HO-3867 and CT + HO-3867 + SH-4-54 all have the same theoretical efficacy. This can be explained by the fact that both the drugs, HO-3867 and SH-4-54, inhibit STAT3 and do not have any other targets in the osteosarcoma pathways.

The cellular apoptosis occurring in ABRAMS OS cells with respect to time is displayed in Fig 8c. As seen in Fig 8c, all drug combinations successfully induce cell death in the OS cells. The biological experiment shows that the action of CT is slightly enhanced by PX-478. The best performing combination is CT with HO-3867 and SH-4-54. The area under the curve for each of the curves in Fig. 8c is plotted in Fig. 8b as a bar graph for ease of comparison.

The results of this experiment show that inhibition of HIF1α could enhance the activity of CT. The Boolean model predicts that the combination of CT with PX-478 is the best combination with two drugs at a time, which implies that HIF1α is a significant intervention point in OS treatment.

3.6 Prediction of Drug Efficacies

The final simulation was performed to test the effect of all possible combinations of faults and drugs with and without Cryptotanshinone. Fig. 9a shows all the drug combinations containing CT and Fig. 9b considers the possible combinations of drugs without CT. The cells that are green indicate high levels of apoptosis (6.5) and the red cells denote low levels of apoptosis (0.3). The fault-free value of apoptosis is 2.23 and with all the faults present, apoptosis drops down
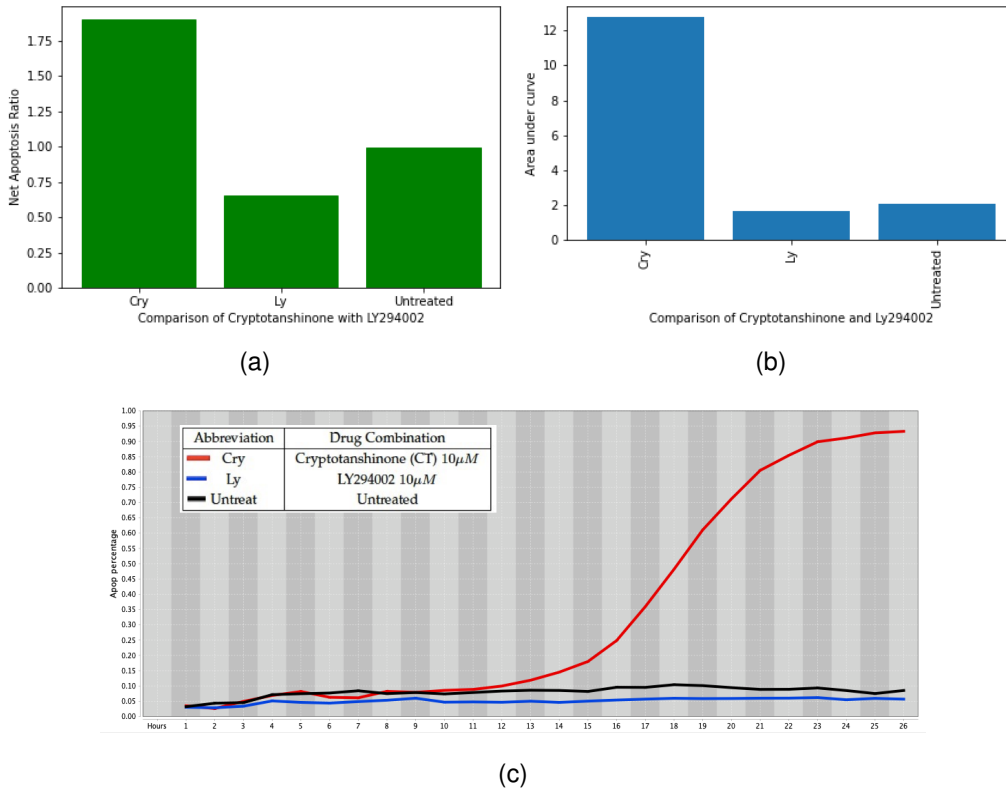
(a)

(b)

(c)

Fig. 6. (a) Simulation results comparing the theoretical efficacy of LY294002 with the theoretical efficacy of CT. The model predicts that CT outperforms LY294002. (b) Area under the curve in Fig. 6c. (c) Experimental results comparing the cellular apoptosis induced by LY294002 and CT. CT outperforms LY294002.
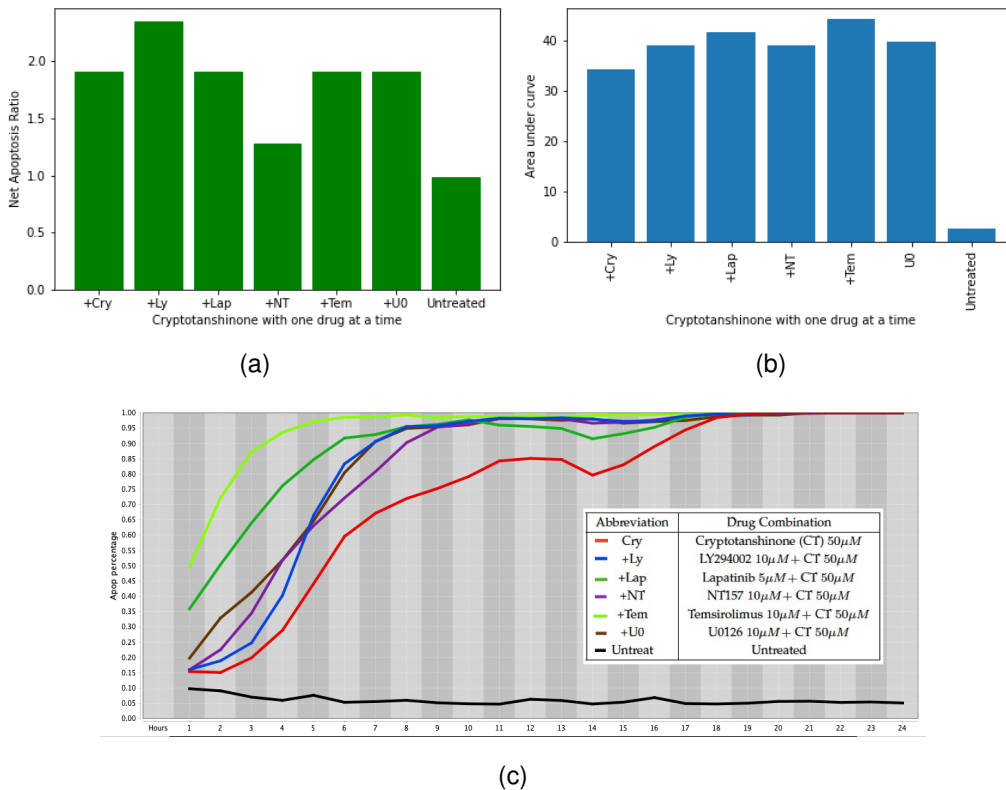

(a)

(b)

(c)

Fig. 7. (a) Simulation results for the theoretical efficacy of each single drug in combination with Cryptotanshinone. CT+LY294002 is the best performing drug combination. (b) Area under the curve in Fig. 7c. (c) Experimental results measuring the cellular apoptosis induced by each single drug in combination with CT. All combinations with CT successfully kill ABRAMS OS cells.
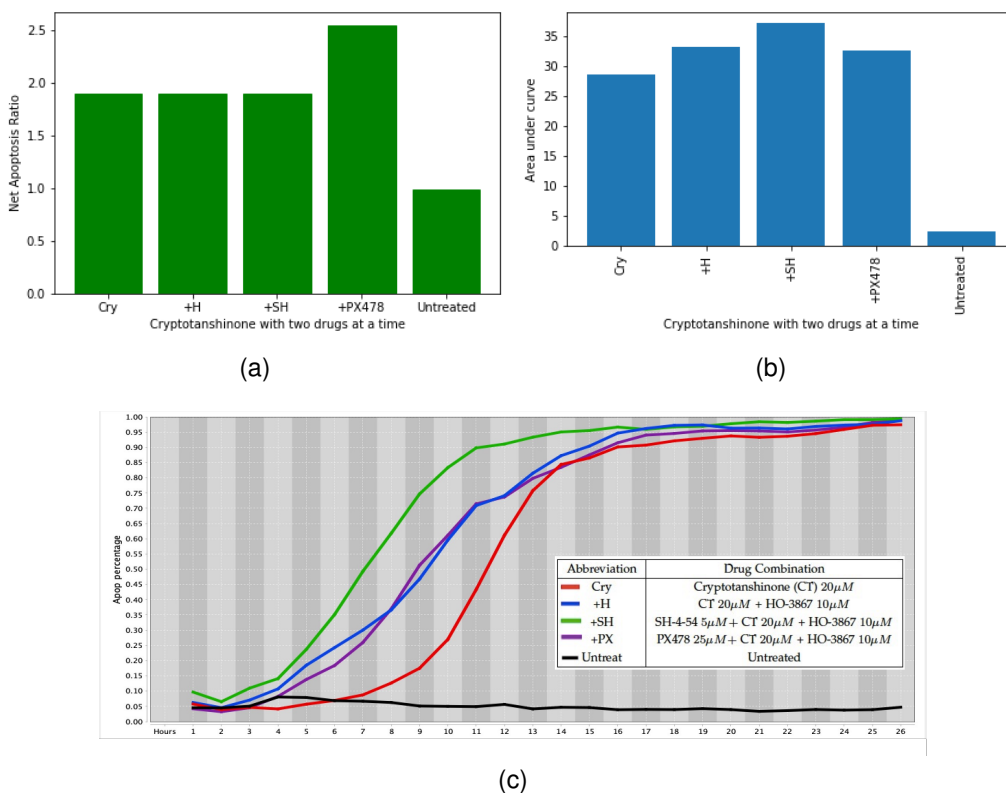
(a)

(b)

(c)

Fig. 8. (a) Simulation results comparing the theoretical efficacy of PX478 in combination with CT and HO-3867 and of SH-4-54 in combination with CT and HO-3867. The model predicts that the apoptosis ratios of CT, CT+HO and CT+HO+SH will be the same. The best performing combination is CT+HO+PX. (b) Area under the curve in Fig. 8c. (c) Experimental results comparing the cellular apoptosis induced by PX478 in combination with both CT and HO-3867 and by SH-4-54 in combination with both CT and HO-3867. All combinations successfully kill ABRAMS OS cells.
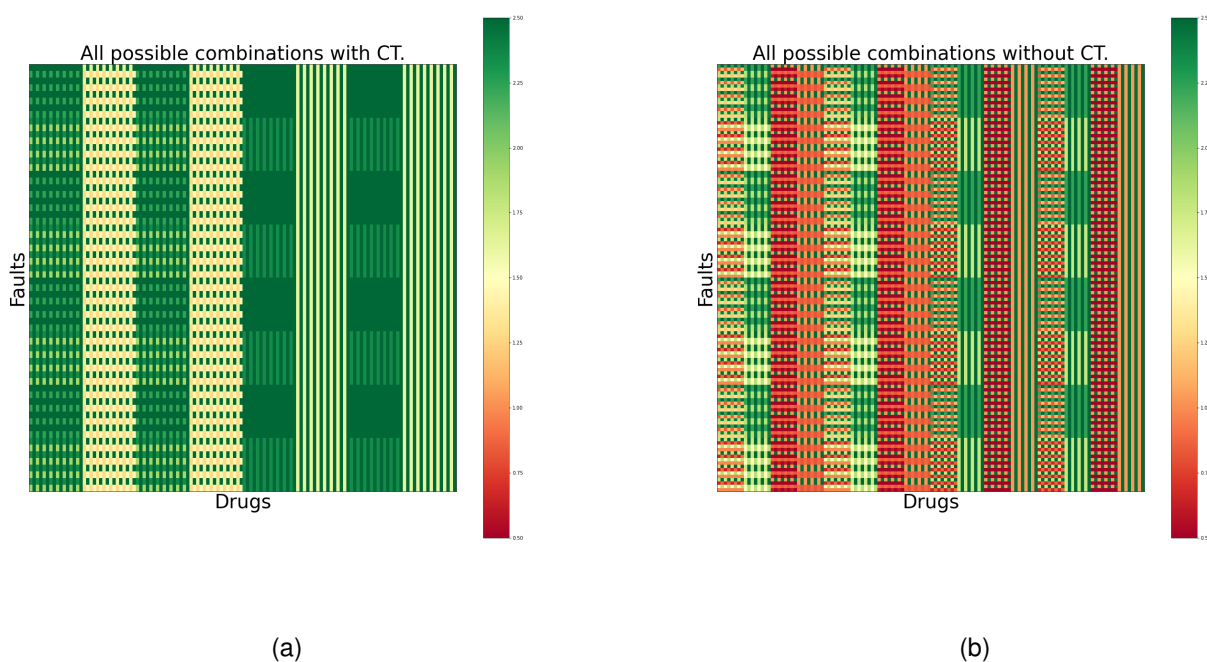

(a)

(b)

Fig. 9. (a) Drug Combinations with Cryptotanshinone. (b) Drug combinations without Cryptotanshinone.

to 0.9. Fig 9b has several red cells, implying that most of the conventional drug combinations fail to induce apoptosis. Without CT, 30% of the drug-fault combinations have a low value of apoptosis (less than 1) and only 38% have a value greater than 2. Fig. 9a has no red cells, which implies that no combination with CT in mix has an apoptosis ratio lower than 1. With Cryptotanshinone, 66% of the drug-fault combinations have a high theoretical efficacy (greater than 2) and the remaining 34% manage to induce apoptosis in osteosarcoma cells with low theoretical efficacy. Our model predicts that every combination with CT should be able to increase TRAIL sensitivity and induce robust cell death in OS cells despite the presence of faults. For a detailed view of the Figures 9a and 9b, refer to the supplementary files.

4 CONCLUSION

We modeled the induction of apoptosis by Cryptotanshinone in OS using a Boolean network. The effects of Cryptotanshinone in combination with other drugs were evaluated. The PI3K/mTOR pathway plays an important role in decreasing TRAIL sensitivity in OS. The results of the simulation indicate HIF1α as a key intervention point in inducing apoptosis in OS cell lines. The theoretically predicted efficacies seem to be in agreement with the experimental results that the action of Cryptotanshinone is enhanced by the drug combinations studied in this paper. Our work shows that the herbal drug Cryptotanshinone is a strong candidate for osteosarcoma treatment.

5 FUTURE WORK

Although we only studied the effect of CT on canine OS cells, the Boolean network model can be used to predict the efficacies of existing and new drugs for human osteosarcoma treatment. New drug combinations can be explored and tested using this model without the overhead of experimentation. Existing biological knowledge is reflected in the Boolean network, and changes or additions to the network can be made easily as and when new knowledge is unearthed. One of the drawbacks of this Boolean network model is it cannot differentiate between drugs with the same genetic targets. However, the Boolean network can be used to identify the genetic target as a key intervention point for therapy.

After the promising results of the in silico modeling are verified by the in vitro experiments on osteosarcoma cell lines, the next step in the drug development process is to prove the efficacy of the drug in a live animal model. The best performing combinations with and without CT can be tested on a mouse model. Further steps would be to experimentally evaluate if the drug combinations are successful when applied to tumor xenografts implanted in mice. The results of the animal model, if successful, would prove the efficacy of CT to induce death in vivo and could serve as the platform based on which Cryptotanshinone could potentially be taken to clinical trials on dogs and on humans.

APPENDIX A
OSTEOSARCOMA BOOLEAN NETWORK MODEL

The simulations were implemented using Python 2.7. The materials supporting the conclusion of this article can be found in the CodeOcean repository https://codeocean.com/capsule/4955422/tree.

ACKNOWLEDGMENTS

REFERENCES

[1] M. Szewczyk, R. Lechowski, and K. Zabielska, "What do we know about canine osteosarcoma treatment? review." *Veterinary Research Communications*, vol. 39, pp. 61–67, 2015.

[2] M. Paoloni, S. Davis, S. Lana, S. Withrow, L. Sangiorgi, P. Picci, S. Hewitt, T. Triche, P. Meltzer, and C. Khanna, "Canine tumor cross-species genomics uncovers targets linked to osteosarcoma progression," *BMC Genomics*, vol. 10, p. 625, 2009.

[3] C. Vogel, A. Chan, B. Gril, S.-B. Kim, J. Kurebayashi, L. Liu, Y.-S. Lu, and H. Moon, "Management of erbb2-positive breast cancer: insights from preclinical and clinical studies with lapatinib." *Japanese Journal of Clinical Oncology*, vol. 40, pp. 999–1013, 2010.

[4] S. L. Fossey, A. T. Liao, J. K. McCleese, M. D. Bear, J. Lin, P.-K. Li, W. C. Kisseberth, and C. A. London, "Characterization of stat3 activation and expression in canine and human osteosarcoma," *BMC Cancer*, vol. 9, p. 81, 2009.

[5] G. Ottaviani and N. Jaffe, "Pediatric and adolescent osteosarcoma," *Cancer Treatment and Research*, vol. 152, pp. 15–32, 2009.

[6] M. S. Isakoff, S. S. Bielack, P. Meltzer, and R. Gorlick, "Osteosarcoma : Treatment and a collaborative pathway to success," *Journal Of Clinical Oncology*, vol. 33, pp. 3029–3035, 2015.

[7] J. J. Morrowa and C. Khannab, "Osteosarcoma genetics and epigenetics: Emerging biology and candidate therapies," *Critical Reviews in Oncogenesis*, vol. 20, pp. 173–197, 2015.

[8] A. Nguyen, V. Nguyen, D. Pham, M. Mravic, M. A. Scott, and A. W. James, "Novel signaling pathways in osteosarcoma," *International Journal of Orthopaedics*, vol. 1, pp. 73–84, 2014.

[9] P. Angulo, G. Kaushik, D. Subramaniam, P. Dandawate, K. Neville, K. Chastain, and S. Anant, "Natural compounds targeting major cell signaling pathways: a novel paradigm for osteosarcoma therapy," *Journal of Hematology & Oncology*, vol. 10, pp. 4649–4653, 2017.

[10] C. Khanna, T. M. Fan, R. Gorlick, L. J. Helman, E. S. Kleinerman, P. C. Adamson, P. J. Houghton, W. D. Tap, D. R. Welch, P. S. Steeg, G. Merlino, P. H. Sorensen, D. G. Kirsch, K. A. Janeway, B. Weigel, R. L. Randall, P. Meltzer, S. J. Withrow, M. Paoloni, R. N. Kaplan, B. A. Teicher, N. L. Seibel, A. Uren, S. R. Patel, J. Trent, S. A. Savage, L. Mirabello, D. Reinke, D. A. Barkauskas, M. Krailo, M. A. Smith, and M. Bernstein, "Toward a drug development path that targets metastatic progression in osteosarcoma." *Clinical Cancer Research*, vol. 20, pp. 4200–4209, 2014.

[11] T.-a. Matsui, Y. Sowa, T. Yoshida, H. Murata, M. Horinaka, M. Wakada, R. Nakanishi, T. Sakabe, T. Kubo, and T. Sakai, "Sulforaphane enhances trail-induced apoptosis through the induction of dr5 expression in human osteosarcoma cells," *Carcinogenesis*, vol. 27, pp. 1768–1777, 2006.

[12] G. Picarda, F. Lamoureux, L. Geffroy, P. Delepine, T. Montier, K. Laud, F. Tirode, O. Delattre, D. Heymann, and F. Rédini, "Preclininal evidence that use of trail in ewing's sarcoma and ostosarcoma therapy inibits tumor growth, prevents osteolysis and increases animal survival," *Clinical Cancer Research*, 2010.

[13] B. Tu, J. Zhu, S. Liu, L. Wang, Q. Fan, Y. Hao, C. Fan, and T.-T. Tang, "Mesenchymal stem cells promote osteosarcoma cell survival and drug resistance through activation of stat3," *Oncotarget*, vol. 7, pp. 48 296–48 308, 2016.

[14] Y. Zhang, S. B. Cabarcas, J. Zheng, L. Sun, L. A. Mathews, X. Zhang, H. Lin, and W. Farrar, "Cryptotanshinone targets tumor-initiating cells through down-regulation of stemness genes expression," *Oncology Letters*, vol. 11, pp. 3803–3812, 2016.

[15] Z. Chen, R. Zhu, C. Zheng, Jiayi Chen, C. Huang, J. Ma, C. Xu, W. Zhai, and J. Zheng, "Cryptotanshinone inhibits proliferation yet induces apoptosis by suppressing stat3 signals in renal cell carcinoma," *Oncotarget*, vol. 8, no. 30, pp. 50 023—-50 033, 2017.

[16] L. Lu, S. Zhang, C. Li, C. Zhou, D. Li, P. Liu, M. Huang, and X. Shen, "Cryptotanshinone inhibits human glioma cell proliferation in vitro and in vivo through shp-2-dependent inhibition of stat3 activation," *Cell Death & Disease*, vol. 8, p. 2767, 2017.

[17] A. K.-W. Tse, K.-Y. Chow, H.-H. Cao, C.-Y. Cheng, H.-Y. Kwan, H. Yu, G.-Y. Zhu, Y.-C. Wu, W.-F. Fong, and Z.-L. Yu, "The herbal compound cryptotanshinone restores sensitivity in cancer cells that are resistant to the tumor necrosis factor-related apoptosis-inducing ligand," *Journal of Cellular Biochemistry*, vol. 288, no. 41, pp. 29 923–29 933, 2013.

[18] H. Nakamura, A. Taguchi, K. Kawana, A. Kawata, M. Yoshida, A. Fujimoto, J. Ogishima, M. Sato, T. Inoue, H. Nishida, H. Furuya, K. Tomio, S. Eguchi, M. Mori-Uchino, A. Yamashita, K. Adachi, T. Arimoto, O. Wada-Hiraike, K. Oda, T. Nagamatsu, Y. Osuga, and T. Fujii, "Stat3 activity regulates sensitivity to tumor necrosis factor-related apoptosis-inducing ligand-induced apoptosis in cervical cancer cells." *International Journal of Oncology*, vol. 49, no. 5, pp. 2155–2162, 2016.

[19] J.-H. Yen, H. S. Huang, C. J. Chuang, and S.-T. Huang, "Activation of dynamin-related protein 1 - dependent mitochondria fragmentation and suppression of osteosarcoma by cryptotanshinone," *Journal of Experimental and Clinical Cancer Research*, vol. 38, no. 2, 2019.

[20] R. S. Saraf, A. Datta, C. Sima, J. Hua, R. Lopes, and M. Bittner, "An in-silico study examining the induction of apoptosis by cryptotanshinone in metastatic melanoma cell lines," *BMC Cancer*, vol. 18, p. 855, 2018.

[21] S. W. G. Tait and D. R. Green, "Mitochondria and cell death: outer membrane permeabilization and beyond," *Molecular Cell Biology*, vol. 11, no. 9, pp. 621–632, 2010.

[22] C. Fleury, B. Mignotte, and J.-L. Vayssière, "Mitochondrial reactive oxygen species in cell death signaling," *Biochimie*, vol. 84, no. 2-3, pp. 131–141, 2002.

[23] N. Corazza, D. Kassahn, S. Jakob, A. Badmann, and T. Brunner, "Trail-induced apoptosis: Between tumor therapy and immunopathology," *Annals of the New York Academy of Science*, vol. 1171, pp. 50—-58, 2009.

[24] S. Jamil, S. Mojtabavi, P. Hojabrpour, S. Cheah, and V. Duronio, "An essential role for mcl-1 in atr-mediated chk1 phosphorylation," *Molecular Biology of the Cell*, vol. 19, no. 8, pp. 3212—-3220, 2008.

[25] J. H. Lin, P. Walter, and B. T. Yen, "Endoplasmic reticulum stress in disease pathogenesis," *Annual Review of Pathology: Mechanisms of Disease*, vol. 3, pp. 399–425, 2008.

[26] M. Kanehisa, M. Furumichi, M. Tanabe, Y. Sato, and K. Morishima, "Kegg: new perspectives on genomes, pathways, diseases and drugs," *Nucleic Acids Research*, vol. 45, no. 1, pp. D353—-D361, 2016.

[27] M. Kanehisa and S. Goto, "Kegg: Kyoto encyclopedia of genes and genomes," *Nucleic Acids Research*, vol. 28, no. 1, p. 27–30, 2000.

[28] D. Olagnier, A. M. Brandtoft, C. Gunderstofte, N. L. Villadsen, C. Krapp, A. L. Thielke, A. Laustsen, and S. Peri, "Nrf2 negatively regulates sting indicating a link between antiviral sensing and metabolic reprogramming," *Nature Communications*, vol. 9, 2018.

[29] R. Layek, A. Datta, M. Bittner, and E. R. Dougherty, "Cancer therapy design based on pathway logic," *Bioinformatics*, vol. 27, no. 4, pp. 548—-555, 2011.

[30] Y. Lu, G.-F. Guan, J. Chen, B. Hu, C. Sun, Q. Ma, Y.-H. Wen, X.-C. Qiu, and Y. Zhou, "Aberrant cxcr4 and β-catenin expression in osteosarcoma correlates with patient survival," *Oncology Letters*, vol. 10, no. 4, pp. 2123—-2129, 2015.

[31] J. Xu, J.-Y. Zhou, W.-Z. Wei, and G. S. Wu, "Activation of the akt survival pathway contributes to trail resistance in cancer cells," *PLOS one*, 2010.

[32] E. Flashner-Abramson, S. Klein, G. Mullin, E. Shoshan, R. Song, A. Shir, Y. Langut, M. Bar-Eli, H. Reuveni, and A. Levitzki, "Targeting melanoma with nt157 by blocking stat3 and igf1r signaling," *Oncogene*, vol. 35, pp. 2675—-2680, 2016.

[33] P. Yue, F. Lopez-Tapia, D. Paladino, Y. Li, C.-H. Chen, T. Hilliard, Y. Chen, M. A. Tius, and J. Turkson, "Hydroxamic acid and benzoic acid-based stat3 inhibitors suppress human glioma and breast cancer phenotypes in vitro and in vivo," *Cancer Research*, vol. 76, no. 3, pp. 652–663, 2016.

[34] F. Chiarini, C. Grimaldi, F. Ricci, P. Tazzari, I. Iacobucci, G. Martinelli, P. Pagliaro, J. McCubrey, S. Amadori, and A. M. Martelli, "Temsirolimus, an allosteric mtorc1 inhibitor, is synergistic with clofarabine in aml and aml leukemia initiating cells," *Blood*, vol. 118, p. 2596, 2011.

[35] M. Y. Koh, T. Spivak-Kroizman, S. Venturini, S. Welsh, R. R. Williams, D. L. Kirkpatrick, and G. Powis, "Molecular mechanisms for the activity of px-478, an antitumor inhibitor of the hypoxia-inducible factor-1alpha," *Molecular Cancer Therapeutics*, vol. 7, no. 1, pp. 90–100, 2008.

[36] M. Kanehisa, Y. Sato, M. Kawashima, M. Furumichi, and M. Tanabe, "Kegg: new perspectives on genomes, pathways, diseases and drugs," *Nucleic Acids Research*, vol. 44, no. 1, pp. D457—-D462, 2016.

[37] M. C. Mendoza, E. E. Er, and J. Blenis, "The ras-erk and pi3k-mtor pathways:cross-talk and compensation," *Trends in Biochemical Sciences*, vol. 36, no. 6, pp. 320–328, 2012.

[38] D. Saleiro and L. C. Platanias, "Intersection of mtor and stat signaling in immunity," *Trends in Immunology*, vol. 36, no. 1, pp. 21–29, 2015.

[39] Y.-H. Lin, B. E. Jewell, J. Gingold, L. Lu, R. Zhao, L. L. Wang, and D.-F. Lee, "Osteosarcoma: Molecular pathogenesis and ipsc modeling," *Trends in Molecular Medicine*, vol. 23, pp. 737–755, 2017.

[40] M. K. Rasmussen, L. Iversen, C. Johansen, J. Finnemann, L. S. Olsen, K. Kragballe, and B. Gesser, "Il-8 and p53 are inversely regulated through jnk, p38 and nf-kappab p65 in hepg2 cells during an inflammatory response," *Inflammation Research*, vol. 57, no. 7, pp. 329–339, 2008.

[41] M. Tajan, A. K. Hock, J. Blagih, N. A. Robertson, C. F. Labuschagne, F. Kruiswijk, T. J. Humpton, P. D. Adams, and K. H. Vousden, "A role for p53 in the adaptation to glutamine starvation through the expression of slc1a3," *Cell Metabolism*, 2018.

[42] S. C. Lu, "Glutathione synthesis," *Biochimica et Biophysica Acta*, vol. 1830, pp. 3143—-3153, 2013.

[43] G. P. Meares, R. Liu, Yudongand Rajbhandari, H. Qin, S. E. Nozell, J. A. Mobley, J. A. Corbett, and E. N. Benvenistea, "Perk-dependent activation of jak1 and stat3 contributes to endoplasmic reticulum stress-induced inflammation," *Molecular and Cellular Biology*, vol. 34, no. 20, pp. 3911—-3925, 2014.

[44] O. A. Timofeevaa, N. Tarasovac, X. Zhang, S. Chasovskikh, A. K. Cheema, H. Wang, M. L. Brown, , and A. Dritschilo, "Stat3 suppresses transcription of proapoptotic genes in cancer cells with the involvement of its n-terminal domain," *Proceedings of the National Academy of Science*, vol. 110, no. 4, pp. 1267–1272, 2013.

[45] J. E. Ziello, I. S. Jovina, and Y. Huanga, "Hypoxia-inducible factor (hif)-1 regulatory pathway and its potential for therapeutic intervention in malignancy and ischemia," *YALE JOURNAL OF BIOLOGY AND MEDICINE*, vol. 80, 2007.

[46] T. W. Kensler, P. A. Egner, A. S. Agyeman, K. Visvanathan, J. D. Groopman, J.-G. Chen, T.-Y. Chen, J. W. Fahey, and P. Talalay, "Keap1-nrf2 signaling: A target for cancer prevention by sulforaphane," *Topics in Current Chemistry*, vol. 329, pp. 163—-177, 2013.

[47] Q. Ma, "Role of nrf2 in oxidative stress and toxicity," *Annual Review of Pharmacology and Toxicology*, vol. 53, pp. 401—-426, 2013.

[48] Y.-G. Ren, K. W. Wagner, D. A. Knee, P. Aza-Blanc, M. Nasoff, and Q. L. Deveraux, "Differential regulation of the trail death receptors dr4 and dr5 by the signal recognition particle," *Molecular Biology of the Cell*, vol. 15, no. 11, pp. 5064—-5074, 2004.

[49] C. Wilson, T. Wilson, P. G. Johnston, D. B. Longley, and D. J. Waugh, "Interleukin-8 signaling attenuates trail- and chemotherapy induced apoptosis through transcriptional regulation of c-flip in prostate cancer cells," *Molecular Cancer Therapeutics*, vol. 7, 2008.

[50] J. Hua, C. Sima, M. Cypert, G. Gooden, S. Shack, L. Alla, E. Smith, J. M. Trent, E. R. Dougherty, and M. L. Bittner, "Tracking transcriptional activities with high-content epifluorescent imaging," *Journal of Biomedical Optics*, vol. 17, p. 046008, 2012.

[51] R. M. Locklin, E. Federici, B. Espina, P. A. Hulley, R. G. G. Russell, and C. M. Edwards, "Selective targeting of death receptor 5 circumvents resistance of mg-63 osteosarcoma cells to trail-induced apoptosis," *Molecular Cancer Therapeutics*, vol. 6, no. 1, pp. 3219–3228, 2007.

Radhika Saraf Radhika Saraf received her B.E degree in Instrumentation and Control Engineering from the Univerity of Pune in 2014, the M.S

and Ph.D degrees in Electrical Engineering from Texas A&M University in 2017 and 2020 respectively. She has authored one conference and one journal paper in the field of Electrical Engineering.

Aniruddha Datta Aniruddha Datta received the B. Tech degree in Electrical Engineering from the Indian Institute of Technology, Kharagpur in 1985, the M.S.E.E. degree from Southern Illinois University, Carbondale in 1987 and the M.S. (Applied Mathematics) and Ph.D. degrees from the University of Southern California in 1991. In August 1991, he joined the Department of Electrical and Computer Engineering at Texas A&M University where he is currently the J. W. Runyon, Jr. '35 Professor II and Director of the Center for Bioinformatics and Genomic Systems Engineering (CBGSE). His areas of interest include adaptive control, robust control, PID control and Genomic Signal Processing. He has authored or coauthored 5 books and over 200 journal and conference papers on these topics. He is a Fellow of IEEE, and has served as an Associate Editor for the IEEE Transactions on Automatic Control (2001-2003), the IEEE Transactions on Systems, Man and Cybernetics-Part B (2005-2006), the IEEE Transactions on Biomedical Engineering (2013-2015), the EURASIP Journal on Bioinformatics and Systems Biology (2007-2016) , the IEEE Journal of Biomedical and Health Informatics (2014-2016), the IEEE/ACM Transactions on Computational Biology and Bioinformatics (2014-2017) and IEEE Access (2013-2020).

Heather Wilson-Robles Dr. Heather Robles received her DVM from the University of Tennessee in 2003. She completed an internship in Small Animal Medicine and Surgery at the University of Minnesota in 2004 and a residency in Medical Oncology at the University of Wisconsin-Madison in 2007. Dr. Robles joined the Veterinary Small Animal Clinical Sciences Department at Texas A&M University in 2007 as a Clinical Assistant Professor, converted to a tenture track position in 2008 and was awarded tenure in 2014 and full professor in 2020. Dr. Robles teaches primarily in the 2nd and 3rd year Veterinary curriculum. Additionally, Dr. Robles teaches fourth year students and house officers in a small group setting in the hospital. Dr. Robles' research has two main foci- bench based discovery targeting tumor initiating cells while exploiting common drugable pathways between canine and human cancers and clinical research using dogs as a model for human pediatric cancer. She has received over $8.1 million in external funding from a variety of sources. She has written 38 peer reviewed publications, 27 book chapters and authored over 40 scientific oral abstracts at national meetings. Dr. Robles was recently awarded the TVMA Medical specialist of the year award and is the President Elect for the Veterinary Cancer Society.